Article ID：**1001-3555(2024)01-0001-06**

CoO_x Particles Anchored on Pd/HAC Catalyst for Enhancing the Acetylene Dicarbonylation Performance

GUO Xian-zhe[1,2], WANG Dong-wei[1,2], ZHANG Xiao-hui[1], MA Zhan-wei[1*], GOU Fa-rong[1], HU Bin[1*]

(1. State Key Laboratory for Oxo Synthesis and Selective Oxidation, Lanzhou Institute of Chemical Physics, Chinese Academy of Sciences, Lanzhou 730000, China; 2. University of Chinese Academy of Sciences, Beijing 100049, China)

Abstract: A series of CoO_x-Pd/HAC catalysts were prepared by $[Pd_2(\mu\text{-}CO)_2Cl_4]^{2-}$ *in situ* formation of Pd nanoparticles by equivalent impregnation method, and their reactivity in acetylene dicarbonylation was investigated. It was found that the 3%Co-Pd/HAC catalyst has the best activity in the acetylene dicarbonylation (acetylene conversion 75.4%, dimethyl maleate selectivity 86.2%). The catalyst was characterized by X-ray diffraction (XRD), hydrogen temperature programmed reduction (H_2-TPR) and transmission electron microscopy (TEM) and more. Moreover, the incorporation of an appropriate amount of metal cobalt oxide could drive electron migration on the surface of palladium nanoparticles, generate more high-valence Pd species, and increase the CO adsorption capacity, drive the dicarbonylation reaction step to $Pd^{\delta+}\leftrightarrow Pd^0$ cycle process, so as to improve the acetylene dicarbonylation reaction activity. After seven cycles of experiments, the Co-Pd/HAC catalyst has a weak deactivation phenomenon, but has no significant effect on the selectivity of dimethyl butene-dicarboxylate.

Key words: acetylene dicarbonylation; heterogeneous catalysis; palladium carbon; dimethyl maleate

CLC number: O643.32 **Document code:** A **DOI:** 10.16084/j.issn1001-3555.2024.01.001

Dimethyl maleate (DMM) is an important chemical intermediate[1]. At present, the synthesis route of dimethyl maleate is mainly maleic anhydride route through esterification with methanol. The industrial production methods of maleic anhydride are benzene oxidation method, butene oxidation method and C4 olefin method[2−3], but the reaction temperature is above 350 ℃. Meanwhile, the energy crisis motivated us to develop a potential route direct synthesis of dicarboxylic acid ester to replace the route of petroleum. Acetylene alkoxycarbonylation is a well-known reaction to synthesize *α,β*-unsaturated carboxylic acids and their derivatives[4]. Thus, acetylene dicarbonylation has gained increasing attention in academic research.

In 1964, Tsuji *et al*. [5] reported a palladium salt-catalyzed carbonylation system. By using C_2H_2 and CO and catalyzed by $PdCl_2$, muconyl chloride was a major product, accompanied by a considerable amount of fumaryl and maleyl chloride. As a result, much effort has been devoted to developing an efficient homogeneous Pd based catalytic system such as $PdCl_2$-thiourea[6], $PdCl_2/HgCl_2$[7], $PdCl_2/SnCl_2$[8], Pd(xantphos)Cl_2[9], $PdCl_2/CuCl_2$/HCl/O_2[10], $PdCl_2/FeCl_3$/ H_2SO_4/O_2[11], $PdBr_2$-LiBr[12], PdI_2/KI[13], $PdCl_2$/KI[14]. However, in homogeneous catalysis system, there are still problems such as difficult catalyst separation, inability to recycle and reuse, and complex product purification and separation process [15]. In 2020, Wei *et al*. [16−17] used Pd(nano-sheet)/AC to catalyze the acetylene dicarbonylation reaction, and obtained the yield of 43.8% and the DMF selectivity of 99%. They also used Pd/*α*-Fe_2O_3 catalyst with highly dispersed Pd clusters to catalyze the acetylene dicarbonylation reaction, obtained about 75% dimethyl fumarate conversion in 80 ℃. The main reason for the increase in reactivity is the SMSI effect of Pd/*α*-Fe_2O_3 catalyst, where electrons are transferred from Pd nanoclusters to *α*-Fe_2O_3 support to generate electron-deficient Pd centers, which promotes $Pd^{\delta+}\leftrightarrow Pd^0$ cycling and thus improves acetylene dicarbonylation reactivity. In 2021, Zhao et al. [18] prepared a series of bimetallic Co/Pd alloy nano-catalysts by one-step reduction method. With acetonitrile as solvent, the total yield was 77.23%. However, the alloy catalyst still has the disadvantages of small specific surface area, active component waste and poor thermal stability.

Herein, we constructed CoO_x-Pd/HAC heterogenous acetylene dicarbonylation catalytic system. As expected, acetylene conversion reached a maximum of 75.4% at 80 ℃, which is three times higher than that of Pd/AC catalyst and the catalyst can be stably recycled 7 times. Moreover, the catalysts surface structure was characterized by TEM, XRD. CO-TPD and H_2-TPR were evaluated the catalysts adsorption and reduction performance. XPS were characterized to the catalysts surface chemical composition.

1 Experimental section

1.1 Chemicals

All chemicals used in the experiments were of analytical grade, purchased from Shanghai Aladdin Industrial Corporation in China, and directly used without further purification. In all

Received date: 2023-09-22; **Revised date:** 2023-10-25.

Foundation: National Natural Science Foundation of China (22102194); Science and Technology Plan of Gansu Province (20JR10RA044, 23JRRA630; 20YF3GA009)) and Youth Innovation Promotion Association of CAS (2022427).

Biography: Guo Xian-zhe, male, born in 1998, master degree candidate, mainly engaged in research of carbonyl synthesis and selective oxidation.

* Corresponding authors. E-mail: zhanweima@licp.cas.cn; hcom@licp.cas.cn, Tel:+86 931 4968258, Fax: +86 931 8277088.

reactions, the purity of all gases used in the experiment was 99.999%, and the resistivity of deionized water was 18.25 MΩ·cm.

1.2 Activated carbon treatment

Firstly, 1.0 g activated carbon (AC) was added into 15 mL HNO_3 (65%~68%), and then stirred at room temperature for 1 h, washed with water and ethanol for three times, dried in an air oven at 70 ℃ for 12 h, the obtained sample was donated as HAC.

1.3 Catalyst preparation

Co/HAC sample were prepared by an impregnation method employing the synthesized HAC as support. Typically, 0.093 g $Co(NO_3)_2$ was dissolved into 10 mL deionized water, added 1 g activated carbon impregnating for 24 h, dried and put it in muffle furnace, reduced at 400 ℃ under H_2 atmosphere for 8 h, the obtained sample was donated as 3%Co/HAC. As the above method, 1%Co/HAC, 5%Co/HAC, 3%Fe/HAC, 3%Mn/HAC and 3%Cu/HAC samples were obtained.

Co-Pd/HAC catalysts were prepared by an *in-situ* growth method employing the synthesized HAC as support. Typically, 1 g 3%Co/HAC was dispersed in a mixture of ethanol (20 mL) and distilled water (3 mL), the suspension was first subjected to sonication treatment for 15 min. Then the $[Pd_2(\mu\text{-}CO)_2Cl_4]^{2-}$ precursor, synthesized as literature method[19], was added dropwise into the above slurry gradually under vigorous stirring, and maintained for another 1 h. After centrifuged, the obtained powder was washed with deionized water thoroughly, and then dried at 80 ℃ in air overnight. The samples were named as 3%Co-Pd/HAC, 1%Co-Pd/HAC, 5%Co-Pd/HAC, 3%Fe-Pd/HAC, 3%Mn-Pd/HAC, and 3%Cu-Pd/HAC, respectively. The nominal Pd mass content is 3% on the basis of support weight.

1.4 Catalyst activity evaluation

The acetylene dicarbonylation reaction was carried out in a 50 mL stainless steel high-pressure reactor, placed in an oil bath and magnetically stirred at a speed of 900 r·min^{-1}. In a typical experiment, 50 mg catalyst, 10 mg KI and 20 mL methanol were put into the reactor, then 0.27 g of acetylene gas, 0.6 MPa O_2, and 4.6 MPa CO was passed into the reactor, stirring at 60 ℃ for 8 h. The quantitative analyze was performed on a Gas Chromatography (GC) (Shimadzu GC-2014C) with a FFAP capillary column (50 m × 0.32 mm × 0.50 μm), using methyl benzoate as an internal standard. Gas Chromatography-Mass Spectrometer (GC-MS) was conducted on an Agilent 7890A-5975C instrument equipped with a HP-5 MS capillary column (30 m × 0.25 mm × 0.25 μm) to analysis the product selectivity.

1.5 Catalyst characterization

Smart lab-SE type X-ray polycrystalline powder diffractometer was used to determine the XRD spectra of the samples. The instrument is characterized by Cu target Kα (λ= 0.154 056 nm) ray, tube voltage 40 kV, tube current 40 mA, scanning range of 5°~80°, scanning speed 0.2(°)·s^{-1}. H_2-TPR on Tianjin Xianquan Instrument Company TP-5 080 automatic multi-purpose adsorption. The sample of 50 mg palladium carbon catalyst was loaded into the quartz tube, and the temperature was raised to 100 ℃ and kept constant temperature for He gas purging and dehydration, and then lowered to room temperature. TPR experiment was carried out under 10%H_2-Ar gas flow rate of 30 mL·min^{-1}, and the temperature was raised to 800 ℃ at 10 ℃·min^{-1}. The hydrogen consumption signal was detected by thermal conductivity. NH_3-TPD is also carried out on the aforementioned automatic multi-purpose adsorption. The sample of 50 mg palladium carbon catalyst was also loaded into the quartz tube, which was heated to 100 ℃ and kept at constant temperature for 1 h for He gas purging and dehydrating. After falling to room temperature, the TPD experiment was carried out under 10%NH_3-Ar air flow with a flow rate of 40 mL·min^{-1}, and the temperature was heated to 800 ℃ at a rate of 10 ℃·min^{-1}. The hydrogen consumption signal was detected by thermal conductivity. X-ray photoelectron spectra were measured by ESCALABXI+ multifunctional photoelectron spectrometer.

2 Results and discussion

Fig. 1(a) shows the XRD patterns of AC, HAC, and Co-Pd/HAC samples, it can be noted that several derivative peaks in HAC were disappeared after treatment with nitric acid, which indicated that crystalline carbons into amorphous carbons or impurities were dissolved. After loading Pd, weak diffraction peaks at 40.1°, 46.1° and 68.1° appeared, which were consistent with the (111), (200) and (220) crystal faces of Pd fcc structure (JCPDS No.46-1043). Moreover, after loading Co, the new diffraction peaks at 36.5°, 42.4°, 61.5° and 20.8°, 42.5° were corresponded to the CoO (JCPDS No.43-1004) and CoO_2 (JCPDS No.89-8399). $NaBH_4$ solution was used to reduce the CoO_x, XRD patterns showed that the two new diffraction peaks of 23.7° and 50.8° generated Co_2B, so that the catalyst 3%Co-Pd/HAC lost the catalytic activity.

Fig. 1(b)−(c) show the TEM and HRTEM of 3%Co-Pd/HAC. The TEM image showed that the Pd nanoparticles and CoO_x particles were evenly dispersed on the surface of HAC support. The morphology of catalyst in dark field can be further observed by STEM-HAADF (Fig. 2(a)). Fig. 2(b)−(f)shows the distribution of each element in the catalyst clearly.

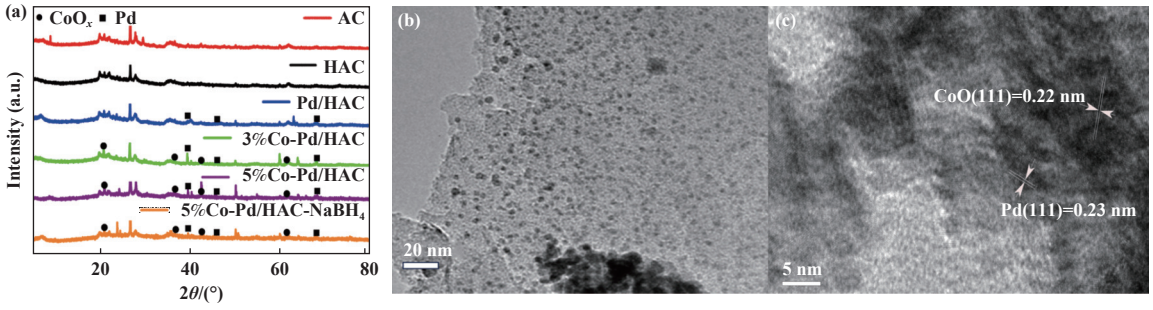

Fig.1 (a) XRD patterns of samples with activated carbon and palladium-carbon catalysts; (b)−(c) TEM image and HRTEM image of Pd nanoparticles and CoO in the Co-Pd/HAC catalyst

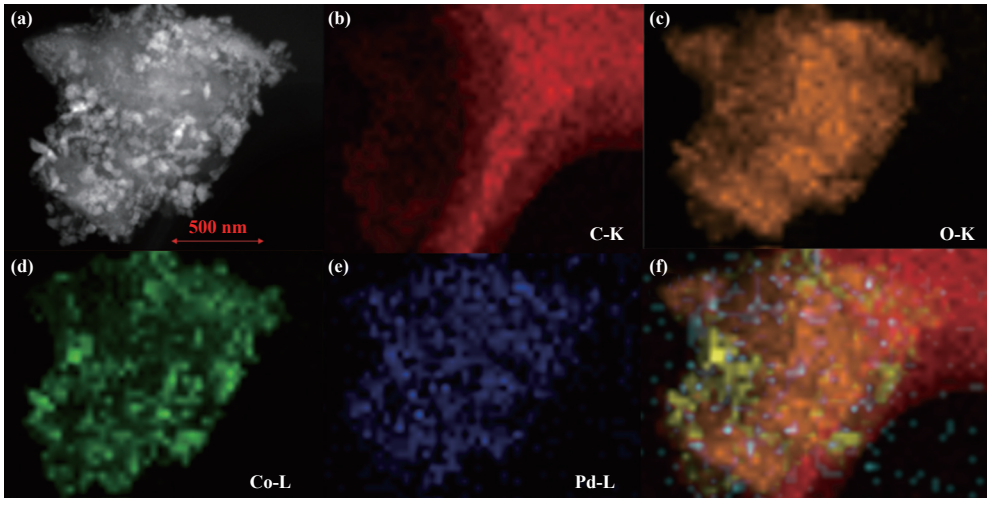

Fig.2 (a) HAADF-STEM image of Co-Pd/AC catalyst; (b)−(e) the resolution elemental mapping of C, O, Co, Pd in Co-Pd/AC catalyst; (f) merging image

The X-ray photoelectron spectroscopy characterization shown in Fig. 3, and it can be noted that the binding energies of Pd 3*d* of 3%Co-Pd/HAC and 5%Co-Pd/HAC catalysts were shifted toward 0.55 eV higher binding energies than Pd/HAC. As shown in Fig. 3(a), the peaks with binding energies at 780.0 and 795.5 eV belong to Co^{2+} $2p_{3/2}$ and Co^{2+} $2p_{1/2}$, respectively, and the peaks at 779.5 and 794.9 eV correspond to Co^{3+} $2p_{3/2}$ and Co^{3+} $2p_{1/2}$, the peaks at 782.5 and 798.0 eV correspond to Co^{4+} $2p_{3/2}$ and Co^{4+} $2p_{1/2}$. The peaks at around 786.5 and 803.0 eV could be ascribed to the satellite peaks[20−21]. The Pd 3*d* XPS spectra of the Co-Pd/HAC is shown in Fig. 3(b), the peaks with binding energies around 334.9 and 340.2 eV belong to Pd^0 $3d_{5/2}$ and Pd^0 $3d_{3/2}$, respectively, and the peaks with binding energies around 336.3 and 341.8 eV belong to Pd^{2+} $3d_{5/2}$ and Pd^{2+} $3d_{3/2}$, the peaks with binding energies around 337.6 and 343.5 eV belong to Pd^{4+} $3d_{5/2}$ and Pd^{4+} $3d_{3/2}$[22]. The incorporation of CoO_x generated more Pd^{4+} and Pd^{2+} species, and the electron deficient Pd species could increase the CO adsorption capacity and improve the reaction activity of the catalyst.

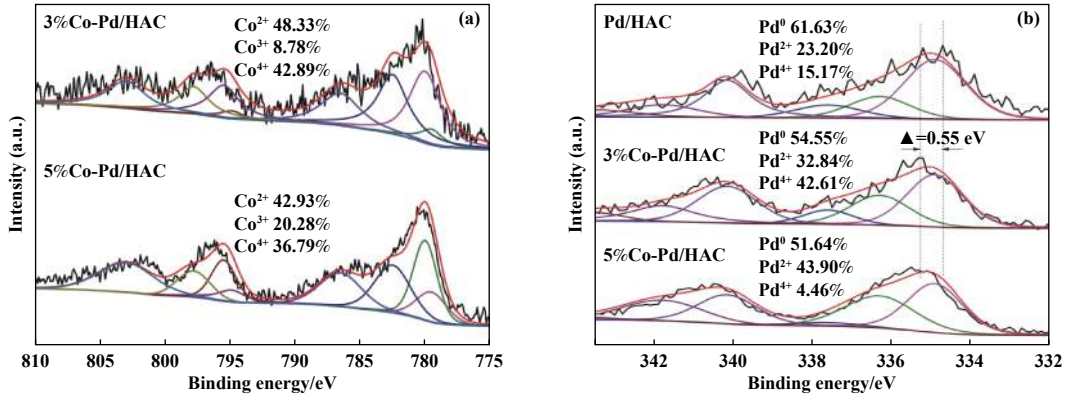

Fig.3 XPS spectra of Co 2*p* (a) and Pd 3*d* (b) of Co-Pd/HAC catalysts

Fig. 4 shows the H_2-TPR spectra of palladium-carbon catalyst and palladium-carbon- cobalt catalyst. After nitric acid treatment, the increase of hydrogen consumption from 400 ℃ is attributed to the increase of oxygen active groups in activated carbon. It can be seen from the spectrum that at around 100 ℃, containing Pd catalysts appear to peaks attributes to the reduction of PdO. After introducing of the additive Co, the oxygen reduction temperature of the in-situ supported palladium nanoparticles on the surface of the palladium carbon catalyst decreases to different degrees at about 300 ℃, which may be because H_2 dissociates into hydrogen on the surface of the Pd nanoparticles[23] and migrates from the surface of the Pd nanoparticles to the surface of the metal Co element. The oxygen active species on the surface of activated carbon were further reduced to form the hydrogen spillover effect, so that the catalyst showed high activity. 400 and 550 ℃ are the reduction peaks of acidic groups and oxygen-containing groups of activated carbon, respectively, while the new peak formed at about 640 ℃ may be the reduction of CoO_x under the action of hydrogen flow. From previous study[24], we indicated $CoO_x \rightarrow Co_3O_4$ (450 ℃), $Co_3O_4 \rightarrow CoO$ (600 ℃), $CoO \rightarrow Co$ (730 ℃).

According to the Fig. 5 CO-TPD test results, CoO_x reduces the desorption temperature of carbon monoxide clearly, and the absolute area of the image is integrated from 400 to 700 ℃ , it can be seen that the surface of the CoO_x catalysts have a higher adsorption capacity of carbon monoxide than the Pd/HAC, indicating that the additive variable valence metals were also the active center to adsorb CO. Moreover, the adsorption of CO

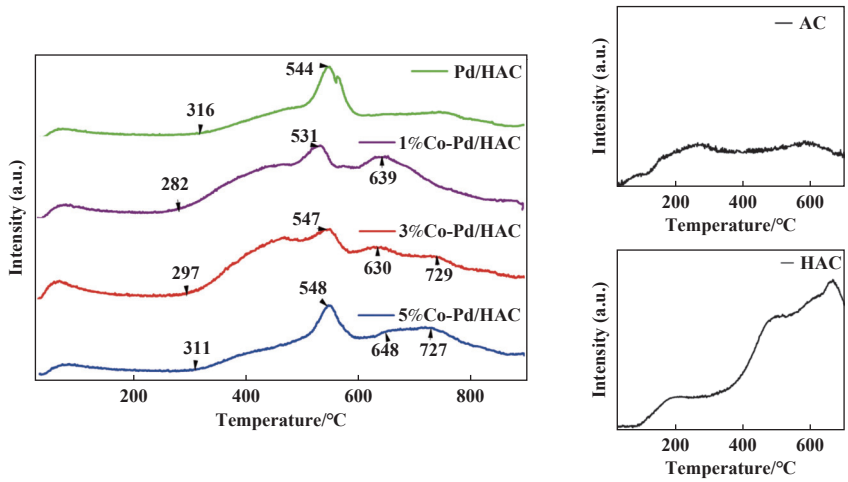

Fig.4 H_2-TPR profiles of Pd/HAC catalysts and different loaded Co of Pd/HAC catalysts

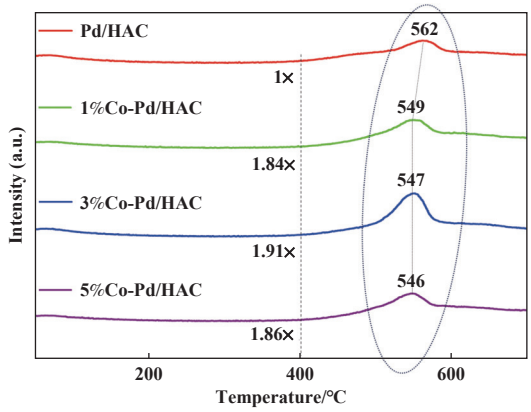

Fig.5 CO-TPD profiles of Pd/HAC and Co-Pd/HAC catalysts

could be contributed to the acetylene di- carbonylation.

Acetylene dicarbonylation was selected as a model reaction, which can be obtained the product dimethyl maleate (DMM) and dimethyl fumarate (DMF). The reaction was conducted under the following conditions: 80 ℃, 4.6 MPa CO and 0.6 MPa O_2, 20 mL methanol and using KI as a promoter, methanol as both a solvent and a nucleophile reagent. Table 1 shows the catalytic performance of different catalysts for acetylene dicarbonylation. It can be seen that Pd/HAC with acetylene conversion 48.6%, which is two times higher than that of Pd/AC (24.0%). After introducing other metal oxides (Co, Fe, Mn, and Cu) into Pd/HAC catalyst, the acetylene conversion furtherly increased. Among them, Co-Pd/HAC catalyst has better catalytic activity and selectivity of dimethyl maleate. Moreover, the effect of the Co amount on the acetylene dicarbonylation activity was investigated. It can be noted 3%Co presented the best catalytic activity and selectivity of dimethyl maleate.

The influence of temperature, time, and gas partial pressure on Co-Pd/HAC catalyst was investigated. As shown in Fig. 6(a), the acetylene conversion increased from 46.5% to 75.4% as the temperature increased from 40 to 80 ℃ and the selectivity of dimethyl maleate is always about 85%. In Fig. 6(b), the acetylene dicarbonylation reaction was complete

Table 1 Catalytic conversion and selectivity of different catalysts in the acetylene dicarbonylation (80 ℃, 5.2 MPa, 20 mL methanol)

Catalyst	Conv./%	DMM Sel./%	DMF Sel./%	Others[a]
Pd/AC	24.0	72.7	25.6	1.7
Pd/HAC	48.6	80.4	19.1	0.5
Co-Pd/HAC	75.4	86.2	13.2	0.6
Fe-Pd/HAC	65.1	81.4	17.9	0.7
Mn-Pd/HAC	62.3	73.1	26.2	0.7
Cu-Pd/HAC	53.3	62.3	37.1	0.6
Pd/CuO	21.5	6.6	85.7	7.7
Pd/MnO_2	17.7	10.5	82.5	7.0
Pd/MgO	trace	–	–	–
1%Co-Pd/HAC	68.3	84.3	14.9	0.8
5%Co-Pd/HAC	71.1	82.5	16.0	1.5
10%Co-Pd/HAC	58.7	81.2	15.7	3.1

a. Contains oxalic acid, dimethyl ester etc.

at about 5 h, and the acetylene conversion rate increased with the progress of the reaction, which may be related to the active site saturation of palladium nanoparticles. In Fig. 6(c), adjusting CO pressure and fixing oxygen pressure, when the total reaction pressure is lower than 5.2 MPa, the conversion increases with the increase of pressure, and then the reaction activity decreases. This may be caused by the reduction of O_2 pressure leading to the weakening of the reaction cycle, because acetylene dicarbonylation is a double cycle process that consumes oxygen, and the reduction of oxygen partial pressure leads to the slowing of the $Pd^{\delta+}\leftrightarrow Pd^0$ cycle [25] and the oxidation cycle of the promoter KI, resulting in the decrease of catalytic activity. Then to evaluate the catalyst recycle stability, the catalytic conditions of 50 mg Co-Pd/HAC,10 mg KI catalyst, 20 mL methanol, 4.6 MPa CO, 0.6 MPa O_2, 6 h under 80 ℃ reaction temperature were adopted. The catalyst after use is washed by deionized water and anhydrous ethanol, dried overnight in an air atmosphere, weighed, and the lost catalyst is supplemented by the side reactor, and then the dicarbonylation reaction continues. The reaction results are shown in Fig. 7(a). It can be found that after several cycles of use of palladium carbon catalyst, acetylene conversion and selectivity decreased to varying degrees, which may be due to the loss of catalyst activity. Some Pd species could no longer complete the reaction cycle, and the particle size of palladium nanoparticles did not change significantly before and after the reaction. However, partial agglomeration of palladium nanoparticles compared with that before the reaction may also be the cause of partial deactivation. Fig. 7(b)−(c) shows the TEM and HRTEM images of the catalyst after the reaction.

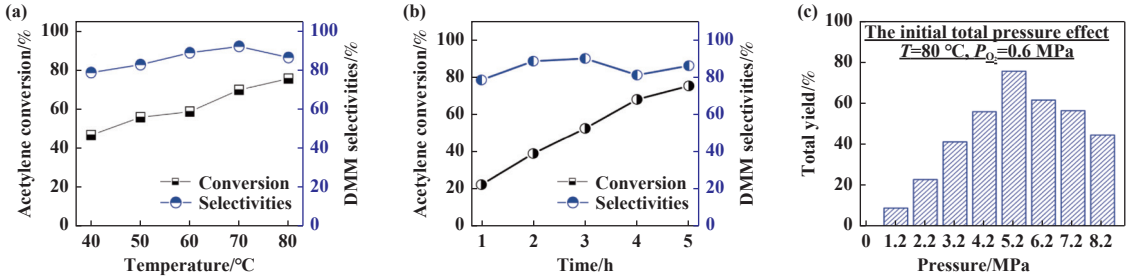

Fig.6 Effects of the reaction parameters on the acetylene dicarbonylation reaction over the Co-Pd/HAC catalyst (Reaction conditions: 0.05 g Co-Pd/HAC catalyst (3%Pd, 3%Co), 0.27 g C_2H_2, 20 mL methanol)

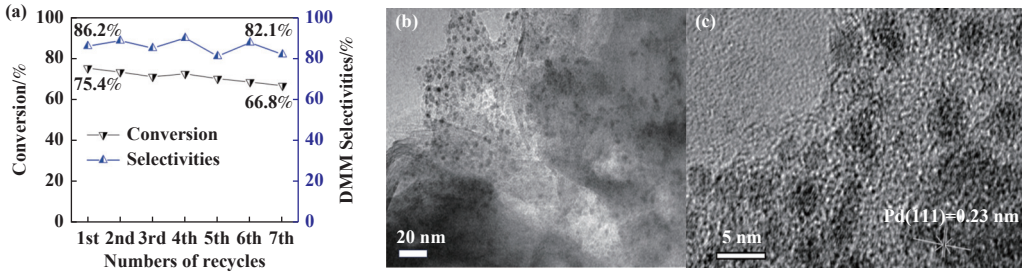

Fig.7 Recycle study of Co-Pd/HAC catalysts (80 ℃ for 6 h) for acetylene dicarbonylation TEM images (b) and HRTEM image (c) of catalysts after acetylene dicarbonylation

3 Conclusion

A series of CoO_x-Pd/HAC catalysts were prepared by $[Pd_2(\mu\text{-}CO)_2Cl_4]^{2-}$ in situ formation of Pd nanoparticles by equivalent impregnation method. It was found that the 3%Co-Pd/HAC catalyst has the best activity in the acetylene dicarbonylation (acetylene conversion 75.4%, dimethyl maleate selectivity 86.2%). Moreover, it was found that the addition of an appropriate amount of metal cobalt oxide could drive electron migration on the surface of palladium nanoparticles, generate electron-deficient Pd species active centers, and drive the cycle of dicarbonylation reaction to step $Pd^{\delta+}\leftrightarrow Pd^0$. CoO_x catalysts have a higher adsorption capacity of carbon monoxide than the Pd/HAC, indicating that the additive variable valence metal oxide were also the active center to adsorption CO for the acetylene dicarbonylation. It has certain research significance to produce *cis*-product dimethyl maleate and *trans*-product dimethyl fumarate directly.

References

[1] Wang Y S, Wu Y X. Study on the synthesis process of dimethyl maleate[J]. *Chem Eng Eq*, 2007, **2007**(4): 13−15+23.

[2] Li X N, Feng Z K, Yang B. Discussion on the production process of maleic anhydride and analysis of current situation [J]. *Tianjin Chem Ind*, 2018, **32**(3): 3−5.

[3] Xue Z Y. *Cis*-anhydride production process and comments on the development of *cis*-anhydride industry in China [J]. *Chem Eng Des*, 1998, **1998**(2): 6−12+3.

[4] Li X J, Feng S Q, Song X G, *et al*. The evolution of single-site Pd_1/AC catalyst during the process of acetylene dialkoxycarbonylation[J]. *J Catal*, 2022, **413**: 762−768.

[5] Takahashi H, Tsuji J. Organic syntheses by means of noble metal compounds: XXXIII. carbonylation of azobenzene-palladium chloride complexes[J]. *J Organomet Chem*, 1967, **10**(3): 511−517.

[6] Cassar L D, Chiusoli G P, Guerrieri F. Synthesis of carboxylic acids and esters by carbonylation reactions at atmospheric pressure using transition metal catalysts[J]. *Synthese*, 1973, **9**: 509−523.

[7] Larock R C. Mercury in organic chemistry. VI. a convenient stere-

ospecific synthesis of *α,β*-unsaturated carboxylic acids and esters *via* carbonylation of vinylmercurials[J]. *J Org Chem*, 1975, **40**: 3237−3242.
[8] Knifton J F. Carboxylation process for preparing alpha unsaturated linear fatty acid derivatives[P]. US: 39.4672, 1975.
[9] Liu H, Lau G P, Dyson P J. Palladium-catalyzed aminocarbonylation of alkynes to succinimides[J]. *J Org Chem*, 2015, **80**: 386−391.
[10] Heck R F. Dicarboalkoxylation of olefins and acetylenes[J]. *J Am Chem Soc*, 1972, **94**(8): 2712−2716.
[11] Xu S Y, Nie Z W, Chen Y D, *et al*. Synthesis of dibutyl ester of butene diacid by the oxidative carbonylation of acetylene [J]. *Chin J Catal* , 1983, **4**(1): 24–30.
[12] Bruk, L G, Kozlova, A P, Marshakha O V, *et al*. New catalytic systems for oxidative carbonylation of acetylene to maleic anhydride[J]. *Russ Chem Bull*, 1999, **48**: 1875−1881.
[13] Bartolo G, Mirco C, Giuseppe S, *et al*. An efficient and selective palladium-catalysed oxidative dicarbonylation of alkynes to alkyloraryl-maleicesters[J]. *J Chem Soc, Perkin Trans 1*, 1994, **1994**(1): 83−87.
[14] Zhao S L, Zhang Q S, Ma Z W, *et al*. Palladium-catalyzed dicarbonylation of acetylene: efficient synthesis of dcarboxylic acid dimethyl esters [J]. *J Mol Catal (China)*, 2017, **31**(5): 411−418.
[15] Liu R, Mu X Y, Xiong X M, *et al*. Research progress of catalysts for acetylene carbonylation[J]. *Natural Gas Chem Ind (C1 Chem Chem Ind)*, 2015, **40**(5): 76−80.
[16] Wei X M, Ma Z W, Mu X Y, *et al*. Catalysts in acetylene carbonylation: from homogeneous to heterogeneous [J]. *Prog Chem*, 2021, **33** (2): 243−253.
[17] Wei X, Ma Z, Lu J, *et al*. Strong metal-support interactions between palladium nanoclusters and hematite toward enhanced acetylene dicarbonylation at low temperature[J]. *New J Chem*, 2020, **44**: 1221−1227.
[18] Zhao J C, Yang Q L, ZhangY C, *et al*. Access to highly active Co/Pd bimetallic nanoparticle catalysts for acetylene dicarbonylation reactions [J]. *Chem Reagents (Beijing, China)*, 2021, **43**(11): 1473−1479.
[19] Li H, Chen G, Yang H, *et al*. Shape-controlled synthesis of surface-clean ultrathin palladium nanosheets by simply mixing a dinuclear Pd(I) carbonyl chloride complex with H_2O[J]. *Angew Chem Int Ed*, 2013, **52**: 8368−8372.
[20] Asif B, Zeeshan M, Iftekhar S, *et al*. Promoted three-way catalytic activity of the Co_3O_4/TiO_2 catalyst by doping of CeO_2 under real engine operating conditions[J]. *Atoms Pollut Res*, 2021, **12**(7): 101088.
[21] Lu J Z, Ma Z W, Wei X M, *et al*. CeO_2 supported NiCo bimetal catalyzes liquid phase hydrogenation of phenol CeO_2 [J]. *J Mol Catal (China)*, 2020, **34**(1): 36−44.
[22] Yaovi H, Christine C, Suzie P, *et al*. High impact of the reducing agent on palladium nanomaterials: new insights from X-ray photoelectron spectroscopy and oxygen reduction reaction[J]. *RSC Adv*, 2016, **6**: 12627−12637.
[23] Acerbi N, Tsang S C, Golunski S, *et al*. A practical demonstration of electronic promotion in the reduction of ceria coated PGM catalysts[J]. *Chem Commun*, 2008, **13**: 1578−1580.
[24] Abdallah I, Christin B, Gamal A, *et al*. Combined TPR, XRD, and FTIR studies on the reduction behavior of Co_3O_4[J]. *Mater Chem Phys*, 2022, **289**: 126367.
[25] Iglesias-Juez A, Kubacka A, Fernández G, *et al*. Nanoparticulate Pd supported catalysts: size-dependent formation of Pd(I)/Pd(0) and their role in CO elimination[J]. *J Am Chem Soc*, 2011, **133**(12): 4484−4489.

CoO_x 引入 Pd/HAC 催化剂增强乙炔双羰化反应活性

郭贤哲[1,2], 王东伟[1,2], 张晓慧[1], 马占伟[1*], 苟发荣[1], 胡 斌[1*]
（1. 中国科学院兰州化学物理研究所 羰基合成与选择氧化国家重点实验室, 甘肃 兰州 730000;
2. 中国科学院大学, 北京 100049）

摘要: 使用 $[Pd_2(\mu\text{-}CO)_2Cl_4]^{2-}$原位生成 Pd 纳米粒子和等体积浸渍法, 制备了一系列 CoO_x- Pd/HAC 催化剂, 并考察了其在乙炔二羰基化反应中的反应活性. 结果表明, 3%Co-Pd/HAC 催化剂在乙炔二羰基化反应中具有最佳活性(乙炔转化率 75.4%, 马来酸二甲酯选择性 86.2%). 采用 X 射线衍射 (XRD)、氢温度程序还原 (H_2-TPR)、透射电镜 (TEM) 等手段对催化剂进行了表征. 适量金属钴氧化物的加入可以驱动钯纳米颗粒表面的电子迁移, 产生更多的高价钯物种, 增强 CO 的吸附能力, 驱动羰基化反应步骤 $Pd^{\delta+}\leftrightarrow Pd^0$ 循环过程, 从而提高乙炔双羰基化反应活性. 经过 7 个循环实验, Co-Pd/HAC 催化剂有微弱失活现象, 但对丁烯二酸二甲酯的选择性没有显著影响.

关键词: 乙炔双羰化; 多相催化; 钯碳; 马来酸二甲酯